FLOW CAMBRIDGE
UNIVERSITY PRESS

RESEARCH ARTICLE

Supplementary Materials
Shear coincidence: implications of the statistics of ocean turbulence microphysics for global diapycnal mixing

A. Mashayek[1]*, B.B. Cael[2], M.H. Alford[3], L. Cimoli[3], and C.P. Caulfield[4]

[1]Imperial College London, London, UK
[2]National Oceanography Centre, Southampton, UK
[3]Scripps Institution of Oceanography, La Jolla, USA
[4]University of Cambridge, Cambridge, UK
*Corresponding author. E-mail: mashayek@ic.ac.uk

Turbulence patch data

The six oceanic datasets employed for the purposes of analyses in Fig 2b and Fig 4b of the main text are the same as those employed by MCA21. Here we provide a brief description and refer to MCA21 for a more comprehensive discussion. The Tropical Instability Wave Experiment (TIWE) dataset includes turbulent patches sampled at the equator at 140^oW in the shear-dominated upper-equatorial thermocline, between 60m and 200m depths, spanning both the upper and lower flanks of the Pacific Equatorial Undercurrent [Lien et al., 1995, Smyth et al., 2001]. The FLUX STAT (FLX91) experiment sampled turbulence at the thermocline (~350-500m depth), in part generated through shear arising from downward-propagating near-inertial waves, about 1000 km off the coast of northern California [Moum, 1996, Smyth et al., 2001]. The IH18 experiment measured full-depth turbulence (up to ~5300m deep) primarily generated by tidal flow over the Izu-Ogasawara Ridge (western Pacific, south of Japan), a prominent generation site of the semidiurnal internal tide that spans the critical latitude of 28.88N for parametric subharmonic instability [Ijichi and Hibiya, 2018]. The Samoan Passage data are measurements of abyssal turbulence generated by hydraulically-controlled flow over sills in the depth range 4500-5500m in the Samoan Passage, an important topographic constriction in the deep limb of the Pacific Meridional Overturning Circulation [see Alford et al., 2013, Carter et al., 2019, we use data from the latter]. The BBTRE data are from turbulence induced by internal tide shear in the deep Brazil Basin (~2500-5000m depth) and were acquired as a part of the original Brazil Basin Tracer Release Expermient (BBTRE; Polzin et al. [1997]), recently re-analyzed by Ijichi et al. [2020]. Also re-analyzed by Ijichi et al. [2020], we use the data from DoMORE which focused on flow over a sill on a canyon floor in the Brazil Basin [Clément et al., 2017, Ijichi et al., 2020].

Dataset	$V(L_O)$	$V(R_{OT})$
Combined	0.021	0.010
BBTRE	0.022	0.028
DoMORE	0.021	0.039
FLX91	0.023	0.015
Hawaii	0.011	0.021
IH18	0.008	0.027
IWISE	0.037	0.033
SP	0.015	0.017
TIWE	0.021	0.031

Table 1. *Kuiper's statistic V for the log-skew-normal approximation of the L_O and R_{OT} distributions of each of the datasets and the combined dataset described in the text.*

Dataset	Exponent	n_{tail} (percentile)	p-value
Combined	2.20 ± 0.01	12519 (80th)	<0.01
BBTRE	2.04 ± 0.03	5754 (73rd)	<0.01
DoMORE	3.27 ± 0.57	178 (98th)	0.08
FLX91	3.85 ± 0.24	598 (82nd)	0.03
Hawaii	2.81 ± 0.12	1010 (90th)	0.09
IH18	2.95 ± 0.05	605 (94th)	**0.13**
IWISE	2.64 ± 0.21	225 (82nd)	0.07
SP	2.57 ± 0.05	3133 (76th)	<0.01
TIWE	3.65 ± 0.53	322 (72nd)	<0.01

Table 2. *Scant evidence for power-law distributions in the Thorpe scale L_T in the datasets used in this study. Left column gives the datasets described in the text and the combined dataset that aggregates all of these. Second column gives the power-law exponent estimate and its uncertainty, as calculated by the method described in Clauset et al. [2009]. The same method selects a minimum L_T value above which a power-law tail is fit; the third column gives the number of samples above, and the percentile above, this minimum L_T value in each case. The fourth column gives the probability that these tail data are power-law distributed, with the p-values above the rule-of-thumb significance criteria of 0.1 suggested by Clauset et al. [2009] in bold. The power-law hypothesis is rejected in all cases except IH18; in this case, the exponent is much steeper (~3) than those described by Smyth et al. [2019] and only ~6% of the data fall into this power-law tail. The cases with borderline p-values (0.1 > p > 0.01) also have steep exponents and/or small tail sample sizes. Altogether these results show that the power-law parameterization is a poor description of the total L_T distribution considered here.*
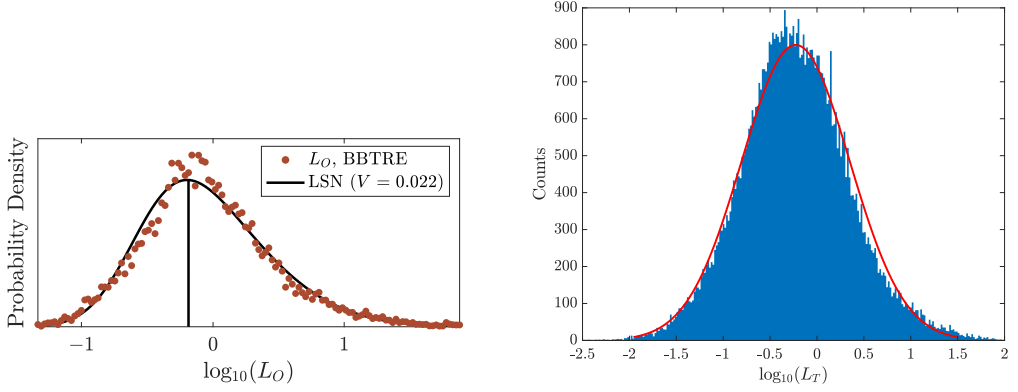
Figure 1. *Left: Log-skew-normal (LSN) fit to L_O data from the Brazil Basin Tracer Release Experiment (BBTRE), shown as probability density. Orange points are the data histogram, with number of bins equal to the (integer-rounded) square root of the sample size. Vertical line added to visualize skewness. V is Kuiper's statistic (see text), evaluated on cumulative probability density. For this log-skew-normal distribution, the log-skewness $\tilde{\mu}_3 = 0.48$. Right: Probability distribution of combined L_T dataset, and the log-normal with the same log-mean and log-standard deviation overlaid.*
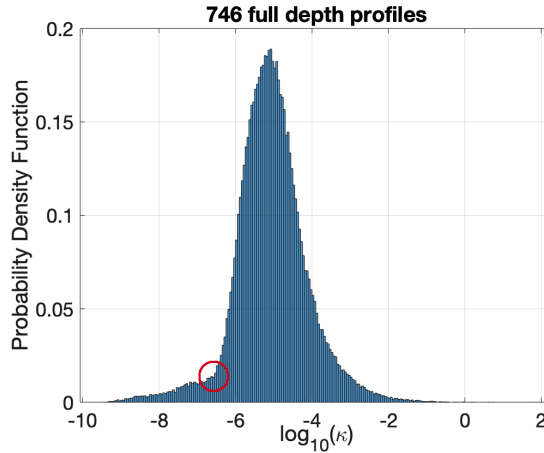

Figure 2. *Probability density function of diffusivity κ for the combined dataset described in the text based on the work of Cael & Mashayek 2021 Cael and Mashayek [2021]. Circle highlights inflection point in cumulative distribution at $10^{-6.5}$ from which we take a background diffusivity $\kappa_{background} \sim 10^{-6.5}$, such that mixing for each patch becomes $M_{background} + M_{patch} = \Gamma_{total}\epsilon = \kappa_{background}N^2 + \Gamma_{param}\epsilon$ and so $\Gamma_{total} = \kappa_{background}N^2 + \Gamma_{param}$, where Γ_{param} is the R_{OT}-parameterized Γ value.*

References

M. H. Alford, J. B. Girton, G. Voet, G. S. Carter, J. B. Mickett, and J. M. Klymak. Turbulent mixing and hydraulic control of abyssal water in the Samoan Passage. *Geophysical Research Letters*, 40(17): 4668–4674, 2013.

B. Cael and A. Mashayek. Log-skew-normality of ocean turbulence. *Physical Review Letters*, 126(22): 224502, 2021.

G. S. Carter, G. Voet, M. H. Alford, J. B. Girton, J. B. Mickett, J. M. Klymak, L. J. Pratt, K. A. Pearson-Potts, J. M. Cusack, and S. Tan. A spatial geography of abyssal turbulent mixing in the samoan passage. Technical Report 4, 2019.

A. Clauset, C. R. Shalizi, and M. E. Newman. Power-law distributions in empirical data. *SIAM review*, 51(4):661–703, 2009.

L. Clément, A. M. Thurnherr, and L. C. St. Laurent. Turbulent mixing in a deep fracture zone on the Mid-Atlantic Ridge. *Journal of Physical Oceanography*, 47(8):1873–1896, 2017. ISSN 15200485. http://dx.doi.org/10.1175/JPO-D-16-0264.1.

T. Ijichi and T. Hibiya. Observed variations in turbulent mixing efficiency in the deep ocean. *Journal of Physical Oceanography*, 48(8):1815–1830, 2018. ISSN 15200485. http://dx.doi.org/10.1175/JPO-D-17-0275.1. URL www.ametsoc.org/PUBSReuseLicenses.

T. Ijichi, L. St. Laurent, K. L. Polzin, and J. M. Toole. How Variable Is Mixing Efficiency in the Abyss? *Geophysical Research Letters*, 47(7):1–9, 2020. ISSN 19448007. http://dx.doi.org/10.1029/2019GL086813.

R.-C. Lien, D. R. Caldwell, M. C. Gregg, and J. N. Moum. Turbulence variability at the equator in the central {P}acific at the beginning of the 1991–1993 {E}l {N}ino. *J. Geophys. Res.: Oceans*, 100 (C4):6881–6898, 1995.

J. N. Moum. Efficiency of mixing in the main thermocline. *J. Geophys. Res.*, 101(C5):12–57, 1996.

K. L. Polzin, J. M. Toole, J. R. Ledwell, and R. W. Schmitt. Spatial variability of turbulent mixing in the abyssal ocean. *Science*, 276(5309):93–96, 1997.

W. Smyth, J. Nash, and J. Moum. Self-organized criticality in geophysical turbulence. *Scientific reports*, 9(1):1–8, 2019.

W. D. Smyth, J. Moum, and D. Caldwell. The efficiency of mixing in turbulent patches: inferences from direct simulations and microstructure observations. *J. Phys. Oceanogr.*, 31:1969–1992, 2001.